·ARTICLES· ·论 著·

Solamargine alleviates liver fibrosis by regulating YAP signaling in hepatic stellate cells

HUANG Ruihua[1], Alshami Mohammed Abdulaziz Yahya Ali[1], ZHU Xiaoyun[1], HU Changping[1, 2]

(1. Xiangya School of Pharmaceutical Sciences, Central South University, Changsha 410013;
2. School of Pharmacy, Changzhi Medical College, Changzhi 046000, China)

ABSTRACT

Objective: Solamargine is a natural compound derived from the traditional Chinese medicinal plant *Solanum nigrum L.*, and exhibits a variety of biological activities, including anti-inflammatory, antimalarial, pro-apoptotic, analgesic, and antitumor effects. However, the role of solamargine in liver fibrosis remains unclear. This study aims to investigate the anti-fibrotic effects and potential mechanisms of solamargine using human hepatic stellate cells (LX-2 cells) and a carbon tetrachloride (CCl_4)-induced mouse model of liver fibrosis.

Methods: LX-2 cells were treated with solamargine (1.25 and 2.50 μmol/L) for 24 h. Cell proliferation was assessed using the cell counting kit-8 (CCK-8) assay. The expression levels of fibrosis-related genes and proteins were detected by real-time quantitative PCR (RT-qPCR) and Western blotting analysis. C57BL/6J mice were randomly divided into a control group, CCl_4 group, CCl_4+0.5 mg/kg solamargine group, and CCl_4+1.0 mg/kg solamargine group. The control group received intraperitoneal injections of olive oil, whereas the CCl_4 and solamargine-treated groups received intraperitoneal injections of CCl_4 3 times per week for 4 weeks to induce liver fibrosis. Meanwhile, the solamargine-treated groups were intraperitoneally administered solamargine at low and high doses every other day. At the end of the experiment, liver tissues and plasma samples were collected for analysis. Hematoxylin and eosin (HE), Sirius Red, Masson trichrome, and α-smooth muscle actin (α-SMA) immunohistochemical staining were performed to evaluate pathological changes and the degree of fibrosis. RT-qPCR and Western blot analysis were used to detect the expression of fibrosis-related genes and proteins. Commercial assay kits were used to measure serum aspartate aminotransferase (AST), alanine aminotransferase (ALT), and hepatic hydroxyproline content. To explore whether solamargine regulates Yes-associated protein (YAP) signaling pathway during liver fibrosis, LX-2 cells were treated with solamargine (1.25 and 2.50 μmol/L) for 24 h. Western blotting analysis was performed to

Date of reception: 2025-12-15

First author: HUANG Ruihua, Email: 257202006@csu.edu.cn, ORCID: 0009-0009-3095-3631

Corresponding author: ZHU Xiaoyun, associate professor, Email: zhuxiaoyun@csu. edu. cn, ORCID: 0009-0009-5719-7354; HU Changping, professor, Email: huchangping@csu.edu.cn, ORCID: 0000-0001-7375-3415

Foundation item: This work was supported by the Natural Science Foundation of Hunan Province (2023JJ20081) and the Young Elite Scientists Sponsorship Program by China Association for Science and Technology (2023QNRC001), China.

Open access: This is an open access article under Creative Commons Attribution-NonCommercial-NoDerivatives 4.0 International (CC BY-NC-ND 4.0) (https://creativecommons.org/licenses/by-nc-nd/4.0/).

©Journal of Central South University (Medical Science). All rights reserved.

detect the expression of large tumor suppressor kinase 1 (LATS1), p-LATS1 (Thr1079), YAP and p-YAP (Ser397), while RT-qPCR was used to determine the mRNA expression levels of *YAP*, *Ctgf*, and *Ankrd1*.

Results: CCK-8 assays showed that treatment with 1.25 and 2.50 μmol/L solamargine for 24 and 48 h significantly reduced the proliferative activity of LX-2 cells compared with the control group (all $P<0.05$). RT-qPCR and Western blotting results demonstrated that, compared with the control group, solamargine treatment significantly reduced the mRNA expression levels of fibrosis-related genes, including *Acta*, *Col1a1*, *TGF-β1*, *Timp1*, and *PDGF-A*, as well as inflammatory cytokines *IL-6* and *TNF-α* (all $P<0.05$). Protein expression levels of smooth muscle actin α (α-SMA) and collagen type I alpha 1 chain (Col1a1) were also significantly downregulated (all $P<0.05$). Compared with the CCl_4 group, mice treated with solamargine exhibited markedly alleviated liver pathological injury and reduced inflammatory cell infiltration. Quantitative analyses of Sirius Red and Masson staining showed significantly decreased collagen deposition areas and reduced hepatic hydroxyproline content (all $P<0.05$). Serum ALT and AST levels were also significantly decreased (all $P<0.05$). In addition, the mRNA expression levels of *Acta* and *Col1a1*, as well as α-SMA protein expression in liver tissues, were significantly reduced (all $P<0.05$). In LX-2 cells, solamargine treatment significantly decreased YAP protein expression ($P<0.05$) and increased p-LATS1 (Thr1079) protein levels ($P<0.05$) compared with the control group. No statistically significant differences were observed in total LATS1 or p-YAP (Ser397) protein expression (all $P>0.05$). Furthermore, the mRNA expression levels of *YAP*, *Ctgf*, and *Ankrd1* were significantly decreased (all $P<0.05$).

Conclusion: Solamargine attenuated liver fibrosis by suppressing YAP signaling and downregulating downstream targets such as *Ctgf* and *Ankrd1*. These findings suggest that solamargine holds promise as a potential antifibrotic therapeutic agent.

KEY WORDS solamargine; YAP signaling pathway; hepatic stellate cells; CCl_4; liver fibrosis

澳洲茄边碱通过调控肝星状细胞YAP信号抗肝纤维化

黄睿华[1]，安沙米[1]，祝小云[1]，胡长平[1,2]

(1. 中南大学湘雅药学院药理学系，长沙 410013；2. 长治医学院药学院，长治 046000)

[摘 要] 目的：澳洲茄边碱是一种天然化合物，来源于传统中药植物龙葵(*Solanum nigrum L.*)，具有多种生物活性，包括抗炎、抗疟、促凋亡、镇痛和抗肿瘤活性等。然而，澳洲茄边碱对肝纤维化的影响尚未明确。本研究旨在采用人肝星状细胞(LX-2细胞)及四氯化碳(carbon tetrachloride，CCl_4)诱导的肝纤维化小鼠模型探究澳洲茄边碱抗肝纤维化的作用和潜在机制。**方法：**采用澳洲茄边碱(1.25、2.50 μmol/L)处理LX-2细胞24 h，细胞计数试剂盒-8(cell counting kit-8，CCK-8)检测细胞增殖活性，实时荧光定量PCR(real-time quantitative PCR，RT-qPCR)和蛋白质印迹法检测肝纤维化标志基因和蛋白质的表达水平。将C57BL/6J小鼠随机分为对照组、CCl_4组、CCl_4+0.5 mg/kg澳洲茄边碱组、CCl_4+1.0 mg/kg澳洲茄边碱组。对照组腹腔注射橄榄油，CCl_4组和澳洲茄边碱处理组连续4周腹腔注射CCl_4(每周3次)以诱导肝纤维化，同时，澳洲茄边碱处理组分别按低、高剂量隔日腹腔注射澳洲茄边碱进行治疗。采集肝脏和血浆进行检测。采用苏木精-伊红(hematoxylin and eosin，HE)、天狼星红、Masson及免疫组织化学染色检测肝脏病理结构改变和纤维化程度，RT-qPCR和蛋白质印迹法检测肝纤维化标志基因和蛋白质的表达水平；采用试剂盒检测血清谷草转氨酶(aspartate aminotransferase，AST)和谷丙转氨酶(alanine aminotransferase，ALT)水平及肝脏羟脯氨酸含量。随后，探讨澳洲茄边碱是否调控肝纤维化过程中Yes相关蛋白(Yes-associated protein，YAP)信号通路。采用澳洲

©Journal of Central South University (Medical Science). All rights reserved.

茄边碱(1.25、2.50 μmol/L)处理LX-2细胞24 h，蛋白质印迹法检测大型肿瘤抑制激酶1(large tumor suppressor kinase 1，LATS1)、p-LATS1(Thr1079)及YAP、p-YAP(Ser397)蛋白的表达，RT-qPCR检测*YAP*、*Ctgf*、*Ankrd1* mRNA的表达。**结果：**CCK-8结果显示，1.25、2.50 μmol/L澳洲茄边碱处理LX-2细胞24 h及48 h后，细胞增殖活力较对照组均显著下降(均P<0.05)。RT-qPCR和蛋白质印迹法结果显示，与对照组比较，澳洲茄边碱处理组纤维化标志基因*Acta*、*Col1a1*、*TGF-β1*、*Timp1*、*PDGF-A*及炎症因子*IL-6*、*TNF-α*的mRNA表达水平均显著降低(均P<0.05)，平滑肌肌动蛋白α(smooth muscle actin α，α-SMA)及I型胶原α1链(collagen type I alpha 1 chain，Col1a1)蛋白表达亦显著下调(均P<0.05)。与CCl_4组相比，CCl_4+澳洲茄边碱组小鼠肝脏病理损伤均明显减轻，炎症细胞浸润均减少；天狼星红和Masson染色定量分析表明，胶原沉积面积均显著减少，肝脏羟脯氨酸含量明显降低(均P<0.05)；血清ALT和AST水平均显著下降(均P<0.05)；同时，肝组织中*Acta*、*Col1a1*的mRNA表达水平及α-SMA的蛋白质表达水平均显著下调(均P<0.05)。在LX-2细胞中，与对照组相比，澳洲茄边碱处理均可显著降低YAP蛋白表达水平(均P<0.05)，同时升高p-LATS1(Thr1079)蛋白水平(P<0.05)；LATS1总蛋白及p-YAP(Ser397)蛋白表达的差异无统计学意义(均P>0.05)；此外，*YAP*、*Ctgf*及*Ankrd1*的mRNA水平均显著下降(均P<0.05)。**结论：**澳洲茄边碱通过抑制YAP表达，下调*Ctgf*和*Ankrd1*表达水平，从而抑制肝纤维化的发生和发展，有望成为抗肝纤维化治疗的潜在候选药物。

[关键词] 澳洲茄边碱；YAP信号通路；肝星状细胞；四氯化碳；肝纤维化

Liver fibrosis is a wound-healing response to chronic hepatic injury of diverse etiologies[1]. This pathological process is defined by the excessive deposition of extracellular matrix (ECM), ultimately leading to serious clinical consequences, including portal hypertension, hepatic failure, and progression to cirrhosis and hepatocellular carcinoma (HCC) [2]. The recent approval of resmetirom and semaglutide has provided new therapeutic options for metabolic dysfunction-associated steatohepatitis (MASH)-associated liver fibrosis[3-4]. Nevertheless, a deeper understanding of the mechanisms underlying fibrogenesis remains critical for development of next-generation anti-fibrotic therapies with superior target specificity and efficacy.

Hepatic stellate cells (HSCs) are recognized as the principal drivers of liver fibrogenesis[5]. In response to liver injury, quiescent HSCs undergo transdifferentiation, a pathological process, into smooth muscle actin α (α-SMA)-positive myofibroblasts[6]. The activated phenotype of HSCs is characterized by robust proliferation and the extensive ECM proteins[7]. In parallel, activated HSCs secrete a broad spectrum of cytokines and chemokines that amplify inflammatory and fibrotic cascade[8]. Consequently, targeting HSCs activation remains a fundamental therapeutic approach in the management of liver fibrosis[1].

The Hippo signaling pathway functions as a pivotal regulatory switch governing HSCs activation[9]. Activation of the Hippo cascade results in phosphorylation of large tumor suppressor kinase (LATS) 1/2, which subsequently phosphorylate the downstream effector Yes-associated protein (YAP). Phosphorylated YAP undergoes cytoplasmic retention or proteasomal degradation, thereby preventing its transcriptional activity. In contrast, hepatic injury suppresses Hippo pathway activity, permitting nuclear translocation of YAP[10]. Within the nucleus, YAP associates with TEA domain (TEAD) family transcription factors to drive the transcriptional program underlying HSCs activation[11]. Consequently, therapeutic interventions aimed at restraining YAP activity—such as by promoting its phosphorylation and degradation—have attracted considerable attention as potential antifibrotic strategies.

Natural compounds derived from medicinal plants play a crucial role in combating liver fibrosis. Among them, solamargine, a steroidal alkaloid glycoside isolated from Lobelia (*Solanum nigrum L.*), exhibits diverse therapeutic applications including antileishmanial activity, antitrypanosomal activity, antitrypanosoma cruzi activity, and notably, potent anticancer effect against various human cancer cell lines[12-14]. Recent research[15] indicated that high concentrations of solamargine were effective in treating HCC by inducing autophagy and apoptosis. Concurrently, low concentrations of solamargine decreased M2 polarization and inhibited epithelial-mesenchymal transition (EMT) of HCC cells. Despite these promising findings, the potential antifibrotic effects of solamargine and its underlying mechanisms remain largely unexplored.

This study aims to evaluate the antifibrotic activity

©Journal of Central South University (Medical Science). All rights reserved.

of solamargine and the underlying mechanisms in cultured human hepatic stellate cells (LX-2 lines) and a carbon tetrachloride (CCl_4)-induced mouse liver fibrosis model.

1 Materials and methods

1.1 Ethics statements

All the animal experiments in this research have been approved by the Ethical Committee of Experimental Animal Welfare of Central South University and conformed to the ethical principles of experimental animal welfare (ethical approval number: CSU-2024-0293).

1.2 Cell culture and treatment

LX-2 cells were cultured in Dulbecco's Modified Eagle Medium (DMEM), supplemented with 10% (vol/vol) fetal bovine serum (FBS) and 100 U/mL penicillin/streptomycin. These cells were grown in a humidified incubator of 5% CO_2 in air at 37 ℃. For cell experiments, LX-2 cells were pretreated with solamargine at 1.25 or 2.50 μmol/L concentrations for 24 h and then collected.

1.3 Animal experiment

Male wild type C57BL/6J mice were bred for 3 d to adapt to the new experimental environment and prepare for animal experiments. Twenty-four mice were randomly divided equally into 4 groups: Control, CCl_4, CCl_4+0.5 mg/kg solamargine, and CCl_4+1.0 mg/kg solamargine groups, n=6 mice per group). To induce liver fibrosis, mice were injected intraperitoneally (i.p.) with 2.5 mL/kg CCl_4 (10% solution in olive oil), 3 times a week for 4 weeks[16]. The control group received i.p. olive oil (same volume as the CCl_4 solution) alone for 4 weeks. The solamargine-treated group were received CCl_4 injection and a concurrent treatment with solamargine (0.5 or 1.0 mg/kg, i.p. every other day) for 4 weeks. Liver tissues and serum were harvested for subsequent experiments.

1.4 In silico ADMET study of solamargine

ADMETlab 3.0 was employed to evaluate ADMET (Absorption, Distribution, Metabolism, Excretion, Toxicity)-related parameters as well as physicochemical properties and medicinal chemistry characteristics of solamargine.

1.5 Luciferase reporter assay

The pGL4.17-collagen type I alpha 1 chain (Col1a1) luciferase reporter plasmid was received as a generous gift from Zhang Hao lab. LX-2 cells were transfected with pGL4.17-Col1a1 luciferase reporter plasmid using the Lipofectamine 3 000 reagent and then treated with solamargine (1.25 or 2.50 μmol/L) for 24 hours. Cells were lysed and subjected to luciferase reporter assay by using Bio-Lite Luciferase Assay System (Vazyme, Nanjing, China; DD1201-01).

1.6 Cell proliferation assay

LX-2 cells were treated with different concentrations of solamargine for 24 or 48 h. Cell proliferation was evaluated by CCK-8 assay (MCE, HY-K0301).

1.7 Real-time quantitative PCR

Total RNA was extracted from the liver tissues of the mice or LX-2 cells using RNA-Quick Purification Kit (Shanghai Yishan Biotechnology) as described by the manufacturer. Complementary DNA (cDNA) synthesis was carried out with HiScript® II Q Select RT SuperMix for qPCR. Real-time quantitative PCR (RT-qPCR) was performed in biological triplicates using SYBR Green reagent (Vazyme, Nanjing, China). The levels of *β-actin* (mouse) or *GAPDH* (human) RNA expression were used to normalize the data. PCR primer sequences are listed in Table 1.

1.8 Western blotting

Proteins were extracted from the liver tissues or HSCs in the lysis buffer consisting of protease inhibitor cocktail and phosphatase inhibitor. The extracted proteins were separated by polyacrylamide sodium dodecylsulfate (SDS) gel and electrophoretically transferred onto polyvinylidene fluoride membranes. The membranes were probed with the indicated antibodies overnight at 4 ℃. Membranes were then incubated with a horseradish peroxidase coupled secondary antibody. Detection was performed using a ChemiDoc XRS+ (Bio-Rad, USA). The relative expressions were quantified densitometrically using the Image Lab Works 4.0 software, and calculated according to the reference bands of anti-β-actin.

©Journal of Central South University (Medical Science). All rights reserved.

Table 1 Primer sequences used for real-time quantitative PCR analysis

Species	Gene	Forward primer(5'−3')	Reverse primer(3'−5')
Human	*Acta*	CCTTGTTTGGGAAGCAAGTGG	TGGAGCTGCTTCACAGGATT
	Col1a1	GTGCGATGACGTGATCTGTGA	CGGTGGTTTCTTGGTCGGT
	YAP	AGCCCAAGAACAGAAAGAACCT	TTGGACAAGTCCAGTGAGGC
	Ctgf	AAGAGAGGGCCCACGTGTA	GAAGGAGCTGTCTGTTCCACA
	Ankrd1	TTCGAGGCACAAGGCACAA	CCATCATTTCACTGGCGAGC
	GAPDH	GACCTGCCGTCTAGAAAAAC	TTGAAGTCAGAGGAGACCAC
Mouse	*Acta*	CCCAGACATCAGGGAGTAATGG	TCTATCGGATACTTCAGCGTCA
	Col1a1	TAAGGGTCCCCAATGGTGAGA	GGGTCCCTCGACTCCTACAT
	β-actin	GGCTGTATTCCCCTCCATCG	CCAGTTGGTAACAATGCCATGT

1.9 Immunofluorescent staining assay

Cell culture slides were blocked by 1% bovine serum albumin (BSA) and incubated with α -SMA antibody (ab7817) overnight at 4 °C. After washing, the slides were incubated for 2 h with Alexa Fluor 647 Donkey anti-Mouse IgG (A-31571). DAPI (Thermofisher, USA; P36966) was used for nuclei staining. Immunofluorescent staining images were obtained by Zeiss LSM800.

1.10 Immunohistochemistry assay

Liver specimens were preserved in 4% paraformaldehyde and then dehydrated in a graded alcohol series. Liver tissues were fixed and embedded in paraffin blocks and cut into 4 μm sections. To examine hepatic morphology and assess liver fibrosis, hematoxylin and eosin (HE), Sirius red and Masson's trichrome staining were performed. Tissue sections were also immunostained for α-SMA. Images were visualized and scanned.

1.11 Serum ALT/AST assay

The serum aspartate aminotransferase (AST)/alanine aminotransferase (ALT) activity was measured according to manufacturer's instruction (Nanjing Jiancheng Bioengineering Institute, C010-2-1, C009-2-1).

1.12 Liver hydroxyproline content assay

Liver hydroxyproline content was determined according to hydroxyproline assay kit's instruction manual (Nanjing Jiancheng Bioengineering Institute, A030-2-1).

1.13 Statistical analysis

All analyses were performed using GraphPad Prism 10 software. All data were expressed as mean± standard deviation (*SD*). Statistical differences between multiple groups of data were analyzed by one-way ANOVA with Bonferroni correction and Student-Newman-Keuls test. $P<0.05$ was considered statistically significant.

2 Results

2.1 In silico ADMET profile of solamargine

The results of ADMET analysis are shown in Figure 1A, Supplement Table 1 and 2 (https://doi.org/10.57760/sciencedb. 35789). The in silico predictions revealed that solamargine possessed excellent human intestinal absorption, favorable plasma protein binding, robust metabolic stability, and low risks for hERG channel inhibition and drug-drug interactions. However, several parameters, including molecular weight, topological polar surface area (TPSA), and permeability indices, fell outside the optimal ranges for standard oral bioavailability. The computational toxicity assessment indicated no acute oral toxicity and minimal central nervous system toxicity, it flagged potential high risks for drug-induced liver injury (DILI) and Ames mutagenicity.

2.2 Solamargine inhibited LX-2 cells proliferation

The CCK-8 assay results showed that solamargine treatment (1.25 or 2.50 μmol/L) significantly inhibited the proliferation of LX-2 cells at both 24 and 48 h (all $P<0.05$, Figure 1B and 1C).

©Journal of Central South University (Medical Science). All rights reserved.

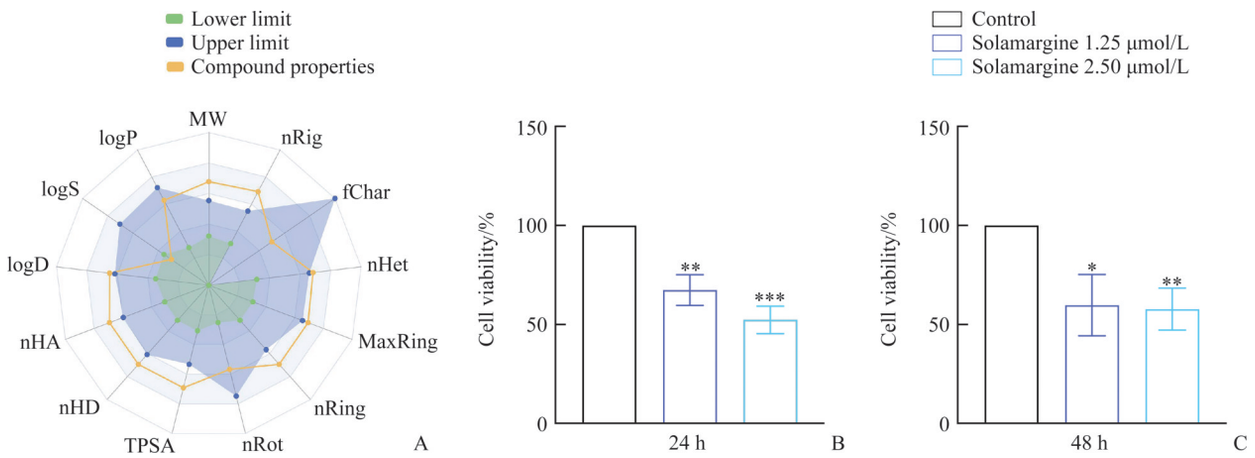


Figure 1 Effect of solamargine on cell proliferation of LX-2 cells

A: ADMET profile of solamargine. B and C: Cell proliferation was determined by CCK-8 assay. LX-2 cells were treated with solamargine (1.25 or 2.50 μmol/L) for 24 (B) or 48 h (C). Data are presented as the means±*SD* (*n*=3). **P*<0.05, ***P*<0.01 vs Control group. ADMET: Absorption, Distribution, Metabolism, Excretion, Toxicity; CCK-8: Cell counting kit-8; *SD*: Standard deviation.

2.3 Solamargine suppressed activation of LX-2 cells

Col1a1 promoter-driven luciferase reporter system revealed that solamargine (1.25 or 2.50 μmol/L) decreased the transcriptional activity of Col1a1 (all $P<0.05$, Figure 2A). Consistently, RT-qPCR results revealed that solamargine significantly decreased profibrogenic genes (*Acta*, *Col1a1*, *TGF-β1*, *Timp1*, and *PDGF-A*) and pro-inflammatory genes (*IL-6* and *TNF-α*) expression (all $P<0.05$, Figure 2B to 2H). Western blotting analysis demonstrated that solamargine significantly reduced profibrogenic proteins (α-SMA and Col1a1) expression (all $P<0.05$, Figure 2I). Immunofluorescence staining also showed a significant attenuation of α-SMA expression by solamargine treatment (both $P<0.05$, Figure 2J). Collectively, these results suggested that solamargine suppressed HSCs activation at both transcriptional and protein levels.

2.4 Solamargine ameliorated CCl_4-induced liver injury in mice

Liver specimens were collected 24 h after the final treatment. Morphological changes in the liver were visualized in sections stained by HE (Figure 3A). Histopathological analysis revealed that the morphological structure of liver tissues in the CCl_4-induced model group exhibited severe disruption, characterized by extensive hepatocellular necrosis, inflammatory cell infiltration, and disorganization of hepatic lobules. Conversely, solamargine treatment ameliorated CCl_4-induced hepatic damage in a dose-dependent manner. Furthermore, serum ALT and AST levels were significantly increased in the CCl_4 group, while solamargine reversed these elevations (all $P<0.05$, Figure 3B). Together, these observations demonstrated that solamargine exerted a hepatoprotective effect against CCl4-induced liver injury.

2.5 Solamargine reduced CCl_4-induced liver fibrosis in mice

Sirius red and Masson's trichrome staining consistently showed that CCl_4 treatment induced remarkable hepatic collagen accumulation compared to the control group (all $P<0.05$, Figure 4A to 4C). This observation was further validated by the assessment of hepatic hydroxyproline levels (Figure 4D). In contrast, solamargine treatment markedly decreased hepatic collagen deposition and hydroxyproline accumulation in the liver fibrosis models (Figure 4A−4D). These results suggest that solamargine effectively mitigated hepatic fibrosis in vivo.

©Journal of Central South University (Medical Science). All rights reserved.

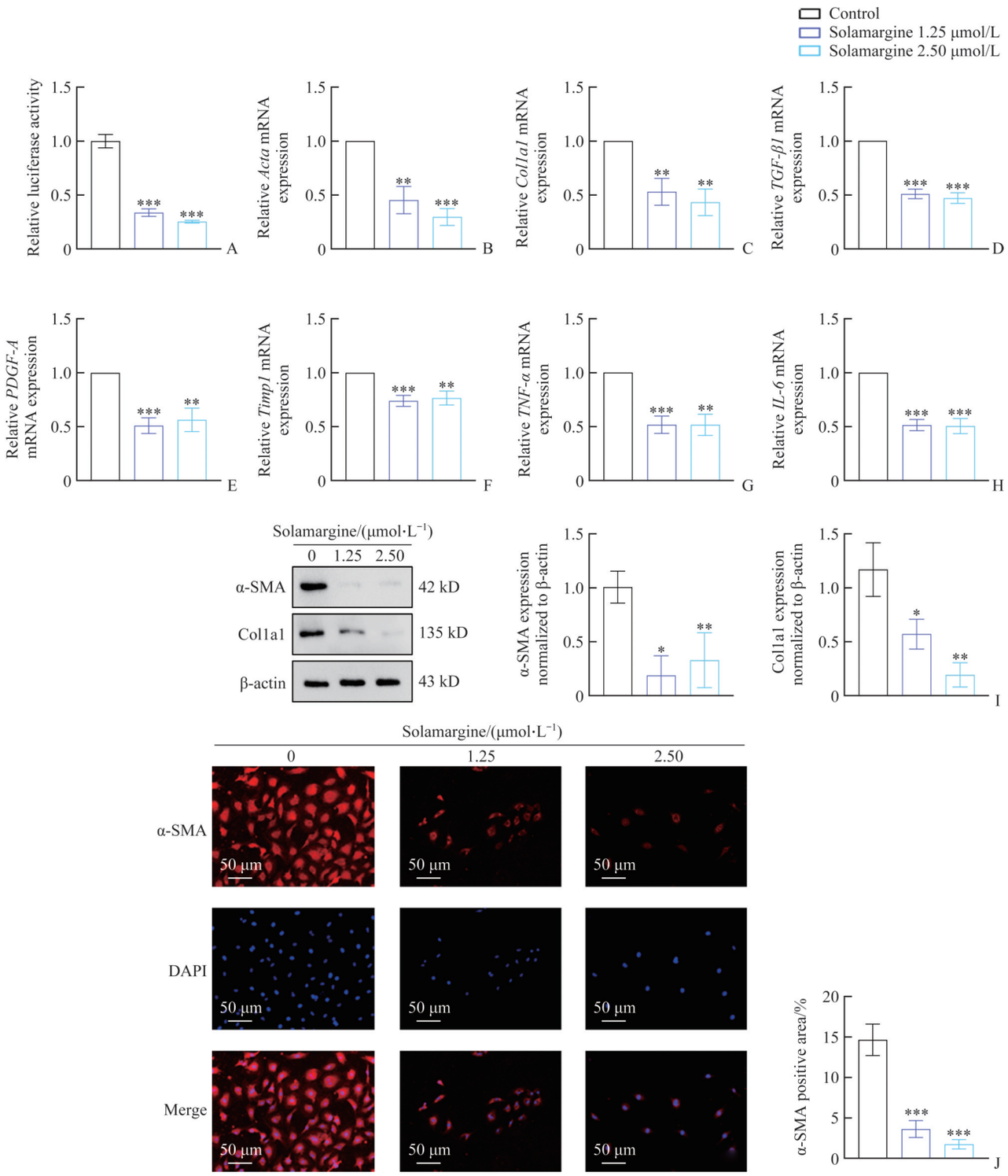


Figure 2 Solamargine reduced activation of LX-2 cells

A: Col1a1 luciferase activity was determined in LX-2 cells transfected with the pGL4.17-Col1a1 luciferase construct. B to H: *Acta* (B), *Col1a1* (C), *TGF-β1* (D), *PDGF-A* (E), *Timp1* (F), *TNF-α* (G), and *IL-6* (H) mRNA levels. The quantitative data for solamargine treatment groups are normalized and expressed as the fold change compared to the control group. I: Representative Western blotting images of α-SMA and Col1a1 protein levels and corresponding quantitative analysis. J: Immunofluorescence staining of α-SMA. LX-2 cells were treated with 1.25 or 2.50 μmol/L solamargine for 24 h. Data are presented as the means±*SD* (n=3). *P<0.05, **P<0.01, ***P<0.001 vs Control group. Acta: Actin alpha, smooth muscle; Col1a1: Collagen type I alpha 1 chain; TGF-β1: Transforming growth factor beta 1; Timp1: TIMP metallopeptidase inhibitor 1; PDGF-A: Platelet derived growth factor subunit A; IL-6: Interleukin-6; TNF: Tumor necrosis factor.

©Journal of Central South University (Medical Science). All rights reserved.

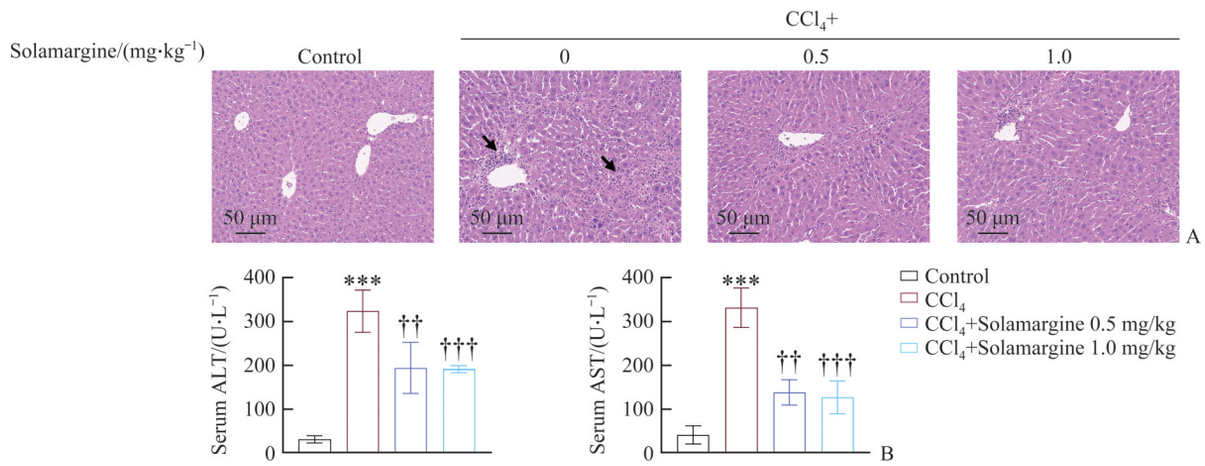


Figure 3 Solamargine ameliorated CCl_4-induced liver injury in mice

A: HE staining. B: Serum ALT and AST levels. Data are presented as the means±*SD* (*n*=6). ***P<0.001 vs Control group; ††P<0.01, †††P<0.001 vs CCl_4 group. CCl_4: Carbon tetrachloride; AST: Aspartate aminotransferase; ALT: Alanine aminotransferase; HE: Hematoxylin and eosin.

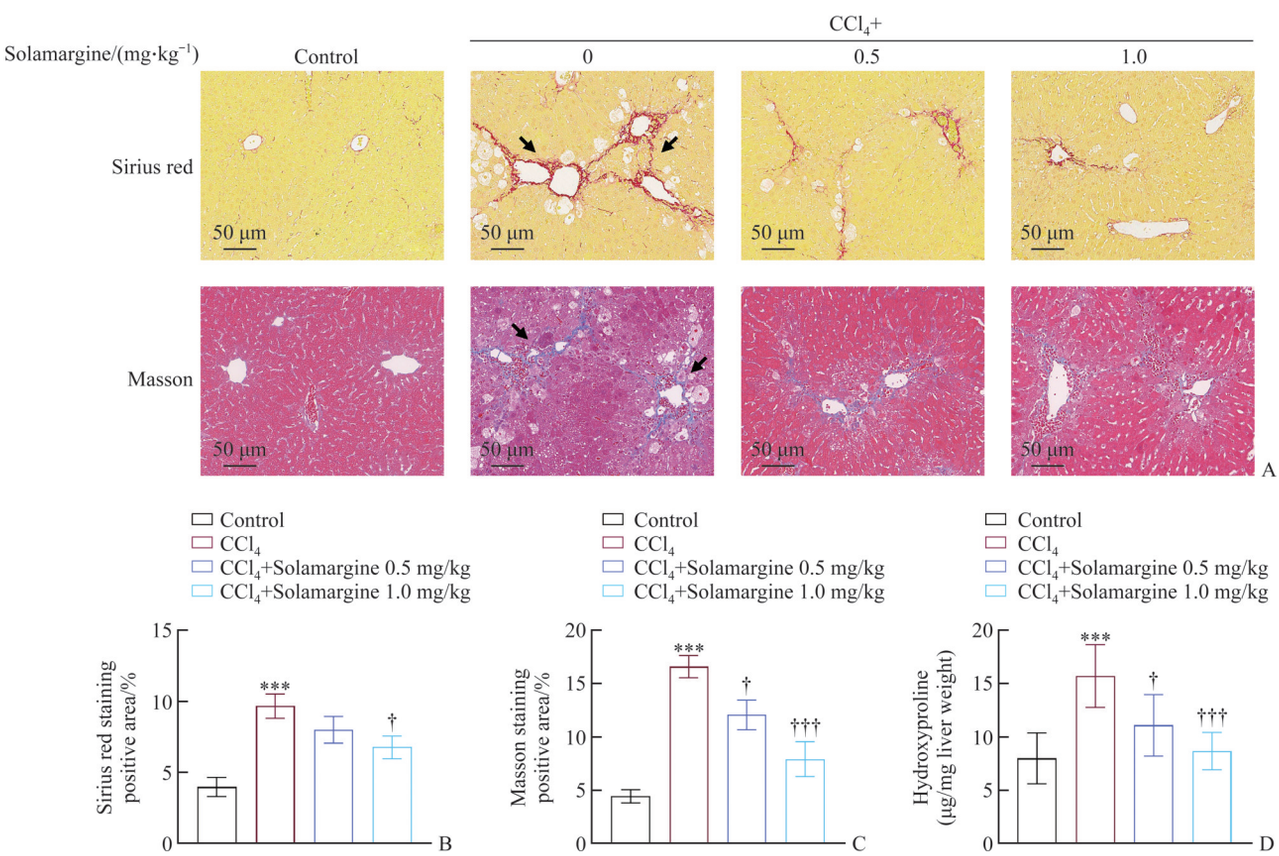


Figure 4 Solamargine ameliorated CCl_4-induced liver fibrosis in mice

A: Sirius red and Masson staining. B and C: Quantification of Sirius red (B) and Masson staining (C). D: Liver hydroxyproline levels. Data are presented as the mean±*SD* (*n*=6). ***P<0.001 vs Control group; †P<0.05, †††P<0.001 vs CCl_4 group.

2.6 Solamargine inhibited HSCs activation in vivo

RT-qPCR revealed that CCl_4 treatment significantly increased the expression of *Acta2* and *Col1a1* compared with controls, whereas solamargine treatment markedly suppressed their expression (all P<0.05, Figure 5A).

©Journal of Central South University (Medical Science). All rights reserved.

Western blotting results showed that α-SMA protein expression was increased in CCl_4-induced fibrotic liver tissue. Solamargine treatment markedly reduced α-SMA protein expression (all P<0.05, Figure 5B and 5C). Similarly, intrahepatic α-SMA expression was significantly increased in mice with liver fibrosis compared to the control group, whereas solamargine treatment attenuated α-SMA expression in the CCl_4 group (Figure 5D). This finding was further confirmed by the quantification of α-SMA-immunopositive areas (all P<0.05, Figure 5E). Collectively, these findings corroborated that solamargine attenuated HSCs activation and fibrogenic progression in vivo.

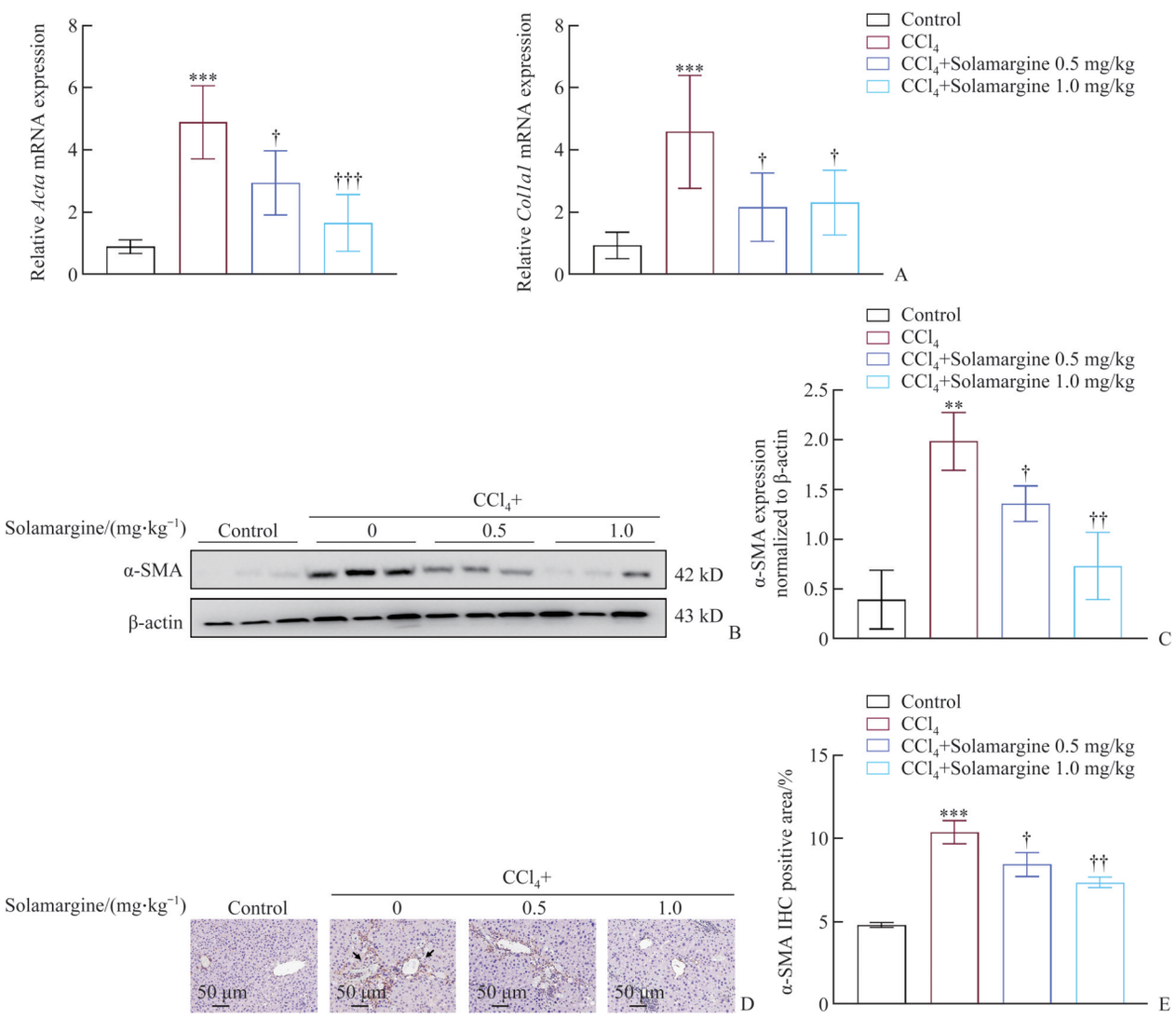


Figure 5 Solamargine inhibited HSCs activation in vivo

A: *Acta* and *Col1a1* mRNA levels. B and C: Representative Western blotting images of α-SMA protein levels and corresponding quantitative analysis. D: α-SMA IHC staining. E: Quantification of α-SMA IHC staining. Data are presented as the mean±*SD* (n=6). **P<0.01, ***P<0.001 vs Control group; †P<0.05, ††P<0.01, †††P<0.001 vs CCl_4 group. HSCs: Hepatic stellate cells; IHC: Immunohistochemistry staining.

2.7 Solamargine inhibited HSCs activation via YAP/Ctgf/Ankrd1 signaling

Western blotting revealed that solamargine decreased total YAP protein levels while increased phosphorylated of LATS1 (p-LATS1, Thr1079) protein levels (all P<0.05). In contrast, no significant changes

©Journal of Central South University (Medical Science). All rights reserved.

were observed in total LATS1 or phosphorylated YAP (p-YAP, Ser397) protein levels (all P>0.05, Figure 6A). At the transcriptional level, solamargine treatment reduced the mRNA levels of *YAP* as well as its downstream target genes *Ctgf* and *Ankrd1* (all P<0.05, Figure 6B). These results suggested that solamargine protected against HSCs activation, at least in part, by inhibiting YAP/cellular communication network factor 2 (Ctgf)/Ankyrin repeat domain 1 (Ankrd1) signaling pathway.

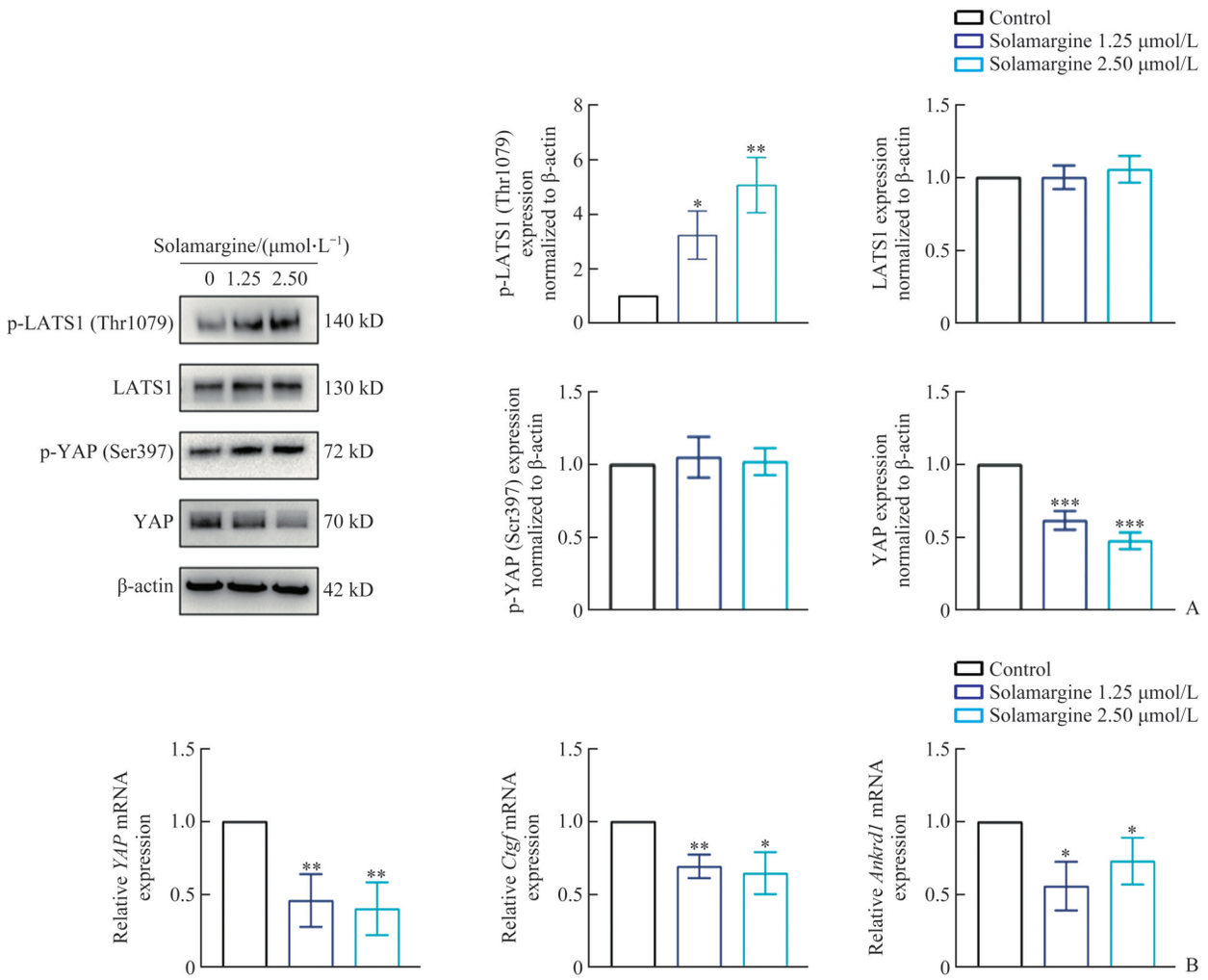


Figure 6 Solamargine inhibited LX-2 cell activation through YAP signaling pathway

A: Representative Western blotting images of LATS1, p-LATS1 (Thr1079), YAP, and p-YAP (Ser397) protein levels and corresponding quantitative analysis. B: *YAP*, *Ctgf*, and *Ankrd1* mRNA levels. The quantitative data for solamargine treatment groups are normalized and expressed as the fold change compared to the control group. LX-2 cells were treated with solamargine for 24 h. Data are presented as the mean±*SD* (n=3). *P<0.05, **P<0.01, ***P<0.001 vs Control group. LATS: Large tumor suppressor kinase 1; YAP: Yes-associated protein; Ctgf: Cellular communication network factor 2; Ankrd1: Ankyrin repeat domain 1.

3 Discussion

Liver fibrosis, a pivotal pathological stage in the progression of chronic liver diseases, poses a severe threat to global health, primarily owing to its potential progression to end-stage liver disease[17, 19]. Despite the recent approval of resmetirom and semaglutide for MASH-related liver fibrosis, there remains an urgent need for more targeted and effective anti-fibrotic therapies[3-4]. The present study systematically explored

©Journal of Central South University (Medical Science). All rights reserved.

the anti-fibrotic effect and underlying mechanism of solamargine, a steroidal glycoside derived from *Solanum nigrum L.*, yielding a coherent line of evidence that supported solamargine as a promising candidate for anti-fibrotic therapy.

First, we evaluated the in silico ADMET profile of solamargine. Solamargine exhibits excellent human intestinal absorption, favorable plasma protein binding, robust metabolic stability, and a low risk for both hERG inhibition and drug-drug interactions, providing a solid pharmacokinetic foundation for its in vivo efficacy. Regarding parameters that fall outside optimal ranges (e.g., high molecular weight, elevated TPSA, and poor permeability), these primarily restrict oral bioavailability[20]. This study utilized intraperitoneal administration, these gastrointestinal absorption barriers were effectively bypassed, thereby minimizing their impact on the observed in vivo pharmacodynamics. Furthermore, computational warnings indicated potential high risks for DILI and AMES mutagenicity. While no overt acute toxicities were observed in mice during our 4-week administration protocol, these in silico predictions represent potential hazards that necessitate rigorous validation through future long-term in vivo toxicology and genotoxicity assays. Based on the above analysis, while the current study establishes a promising proof-of-concept for its anti-fibrotic efficacy, a systematic and comprehensive evaluation of its safety profile remains an essential prerequisite before solamargine can be advanced as a viable clinical candidate.

In vitro findings revealed that solamargine significantly suppressed the proliferation and activation of human hepatic stellate cells (LX-2). The inhibitory effect was evidenced by the marked decrease in the expression of key profibrogenic genes and proteins, including *Acta* (α-SMA), *Col1a1*, *TGF-β1*, *Timp1*, and *PDGF-A*. Moreover, solamargine also mitigated the expression of pro-inflammatory cytokines, such as *IL-6* and *TNF-α*, indicating a dual anti-fibrotic and anti-inflammatory effect. Results from the cell experiments were compellingly validated in a CCl_4-induced mouse model of liver fibrosis. Solamargine administration not only ameliorated hepatic damage, as indicated by reduced serum ALT and AST levels, but also significantly diminished hepatic collagen deposition, as confirmed by Sirius Red and Masson trichrome staining and hydroxyproline quantification. Reduced hepatic α-SMA expression further corroborated its ability to suppress HSCs activation in vivo.

A particularly novel aspect of this work is the mechanistic insight into the role of the Hippo-YAP signaling axis. The Hippo pathway, particularly its downstream effector YAP, is a critical regulator of HSCs activation[10]. Our results demonstrated that solamargine enhanced phosphorylation of LATS1, a crucial upstream kinase in the Hippo cascade, leading to suppression of total YAP protein and downregulation of canonical YAP target genes (*Ctgf* and *Ankrd1*) [21]. Above findings suggested that solamargine inhibited HSCs activation by promoting YAP degradation. This observation is consistent with previous reports[18] that certain natural compounds exerted antifibrotic effects through modulating the YAP pathway. An intriguing observation was the lack of a significant change in p-YAP (Ser397) despite increase p-LATS1 (Thr1079) level. The regulation of YAP phosphorylation by LATS1 exhibits clear asynchrony. Specifically, Ser397 is a secondary phosphorylation site; once phosphorylated, p-YAP (Ser397) is rapidly recognized by the $SCF^{\beta\text{-}TRCP}$ ubiquitin ligase complex and degraded via the proteasome pathway[9, 22]. This process results in extremely low steady-state levels of p-YAP (Ser397) within the cell. We acknowledge that without treating the cells with a proteasome inhibitor (e.g., MG132) to prevent this rapid degradation, this remains a hypothesis requiring future proteasomal inhibition validation. Nevertheless, the significant reduction in total YAP protein and its downstream targets (Ctgf and Ankrd1) directly demonstrates the functional inhibition of YAP resulting from Hippo pathway activation.

This study has certain limitations that warrant further investigation. First, because solamargine was co-administered during the CCl_4 induction phase, our model demonstrated its preventive/prophylactic capability rather than its ability to reverse pre-existing fibrosis. A sequential model—administering solamargine only after fibrosis establishment—is necessary to evaluate true therapeutic reversal efficacy. Second, our current data primarily demonstrate the inhibitory effect of solamargine on activated HSCs, while its impact on strictly quiescent HSCs remains unexplored. Because

©Journal of Central South University (Medical Science). All rights reserved.

YAP expression is inherently low in quiescent HSCs but significantly upregulated during activation, we hypothesize that the YAP-dependent pharmacological efficacy of solamargine would be substantially less pronounced in the resting state[11]. Subsequent studies utilizing freshly isolated primary murine and human HSCs are required to directly evaluate the drug's effect on quiescent HSCs and ensure physiological relevance. Third, the absence of direct genetic interventions means we cannot definitively establish causality between YAP inhibition and the anti-fibrotic effect. Our follow-up research will employ YAP small interfering RNA to silence endogenous YAP, transfect constitutively active YAP mutants (e. g., YAP-5SA), and establish liver fibrosis models in HSCs-specific YAP conditional knockout mice to definitively verify this functional requirement. It is also worth noting that while solamargine exhibited potent anti-fibrotic effects overall, a strictly linear dose-response relationship was not prominent across all evaluated parameters. For certain molecular markers, the high-dose group did not exhibit a proportionally enhanced effect compared to the low-dose group. This phenomenon suggests that the lower dose of solamargine may have already reached a plateau of pharmacological efficacy for these specific targets[23]. Addressing these gaps will be crucial for advancing solamargine toward clinical translation.

Taken together, this study highlights solamargine as a promising therapeutic candidate with the potential to expand the current landscape of antifibrotic treatments. This study provides compelling evidence demonstrating that solamargine suppressed liver fibrosis by modulating Hippo pathway and suppressing YAP/Ctgf/Ankrd1 activity.

Acknowledgements: We sincerely thank the Department of Laboratory Animals of Central South University for providing professional services and support, which provided an important guarantee for this study.

Contributions: HUANG Ruihua Conceptualization, data curation, formal analysis, visualization, original draft writing; Mohammed Abdulaziz Yahya Ali Alshami Data curation, formal analysis; ZHU Xiaoyun and HU Changping Conceptualization, writing review and editing, study supervision, project administration. The final version of the manuscript has been read and approved by all authors.

Conflict of interest: The authors declare that they have no conflicts of interest to disclose.

References

[1] Kisseleva T, Brenner D. Molecular and cellular mechanisms of liver fibrosis and its regression[J]. Nat Rev Gastroenterol Hepatol, 2021, 18(3): 151-166. https://doi.org/10.1038/s41575-020-00372-7.

[2] Sharma S, Le Guillou D, Chen JY. Cellular stress in the pathogenesis of nonalcoholic steatohepatitis and liver fibrosis [J]. Nat Rev Gastroenterol Hepatol, 2023, 20(10): 662-678. https://doi.org/10.1038/s41575-023-00832-w.

[3] Keam SJ. Resmetirom: first approval[J]. Drugs, 2024, 84(6): 729-735. https://doi.org/10.1007/s40265-024-02045-0.

[4] Sanyal AJ, Newsome PN, Kliers I, et al. Phase 3 trial of semaglutide in metabolic dysfunction-associated steatohepatitis [J]. N Engl J Med, 2025, 392(21): 2089-2099. https://doi.org/10.1056/NEJMoa2413258.

[5] Kisseleva T, Ganguly S, Murad R, et al. Regulation of hepatic stellate cell phenotypes in metabolic dysfunction-associated steatohepatitis[J]. Gastroenterology, 2025, 169(5): 797-812. https://doi.org/10.1053/j.gastro.2025.03.010.

[6] Tsuchida T, Friedman SL. Mechanisms of hepatic stellate cell activation[J]. Nat Rev Gastroenterol Hepatol, 2017, 14(7): 397-411. https://doi.org/10.1038/nrgastro.2017.38.

[7] Higashi T, Friedman SL, Hoshida Y. Hepatic stellate cells as key target in liver fibrosis[J]. Adv Drug Deliv Rev, 2017, 121: 27-42. https://doi.org/10.1016/j.addr.2017.05.007.

[8] Taru V, Szabo G, Mehal W, et al. Inflammasomes in chronic liver disease: Hepatic injury, fibrosis progression and systemic inflammation[J]. J Hepatol, 2024, 81(5): 895-910. https://doi.org/10.1016/j.jhep.2024.06.016.

[9] Russell JO, Camargo FD. Hippo signalling in the liver: role in development, regeneration and disease[J]. Nat Rev Gastroenterol Hepatol, 2022, 19(5): 297-312. https://doi.org/10.1038/s41575-021-00571-w.

[10] Liu Y, Lu T, Zhang C, et al. Activation of YAP attenuates hepatic damage and fibrosis in liver ischemia-reperfusion injury [J]. J Hepatol, 2019, 71(4): 719-730. https://doi.org/10.1016/j.jhep.2019.05.029.

[11] Du K, Maeso-Díaz R, Oh SH, et al. Targeting YAP-mediated HSC death susceptibility and senescence for treatment of liver fibrosis[J]. Hepatology, 2023, 77(6): 1998-2015. https://doi.org/10.1097/HEP.0000000000000326.

[12] Kalalinia F, Karimi-Sani I. Anticancer properties of solamargine: a systematic review[J]. Phytother Res, 2017, 31 (6): 858-870. https://doi.org/10.1002/ptr.5809.

©Journal of Central South University (Medical Science). All rights reserved.

[13] Hasan K, Sabiha S, Islam N, et al. Ethnomedicinal usage, phytochemistry and pharmacological potential of *Solanum surattense* burm. f[J]. Pharmaceuticals (Basel), 2024, 17(7): 948. https://doi.org/10.3390/ph17070948.

[14] Borsoi FT, Pastore GM, Arruda HS. Health benefits of the alkaloids from lobeira (*Solanum lycocarpum* St. hill): a comprehensive review[J]. Plants (Basel), 2024, 13(10): 1396. https://doi.org/10.3390/plants13101396.

[15] Yin S, Jin W, Qiu Y, et al. Solamargine induces hepatocellular carcinoma cell apoptosis and autophagy via inhibiting LIF/miR-192-5p/CYR61/Akt signaling pathways and eliciting immunostimulatory tumor microenvironment[J]. J Hematol Oncol, 2022, 15(1): 32. https://doi.org/10.1186/s13045-022-01248-w.

[16] Kong M, Zhou J, Kang A, et al. Histone methyltransferase Suv39h1 regulates hepatic stellate cell activation and is targetable in liver fibrosis[J]. Gut, 2024, 73(5): 810-824. https://doi.org/10.1136/gutjnl-2023-329671.

[17] Younesi FS, Miller AE, Barker TH, et al. Fibroblast and myofibroblast activation in normal tissue repair and fibrosis[J]. Nat Rev Mol Cell Biol, 2024, 25(8): 617-638. https://doi.org/10.1038/s41580-024-00716-0.

[18] Miao H, Wu X, Zhang D, et al. Deciphering the cellular mechanisms underlying fibrosis-associated diseases and therapeutic avenues[J]. Pharmacol Res, 2021, 163: 105316. https://doi.org/10.1016/j.phrs.2020.105316.

[19] Devarbhavi H, Asrani SK, Arab JP, et al. Global burden of liver disease: 2023 update[J]. J Hepatol, 2023, 79(2): 516-537. https://doi.org/10.1016/j.jhep.2023.03.017.

[20] van de Waterbeemd H, Gifford E. ADMET in silico modelling: towards prediction paradise?[J]. Nat Rev Drug Discov, 2003, 2(3): 192-204. https://doi.org/10.1038/nrd1032.

[21] Ma SH, Meng ZP, Chen R, et al. The hippo pathway: biology and pathophysiology[J]. Annu Rev Biochem, 2019, 88: 577-604. https://doi.org/10.1146/annurev-biochem-013118-111829.

[22] Zhang Z, He P, Yang L, et al. Posttranslational modifications of YAP/TAZ: molecular mechanisms and therapeutic opportunities[J]. Cell Mol Biol Lett, 2025, 30(1): 83. https://doi.org/10.1186/s11658-025-00760-4.

[23] Shah M, Rahman A, Theoret MR, et al. The drug-dosing conundrum in oncology-when less is more[J]. N Engl J Med, 2021, 385(16): 1445-1447. https://doi.org/10.1056/NEJMp2109826.

(Edited by TIAN Pu)

©Journal of Central South University (Medical Science). All rights reserved.